Climate change in the Blue Nile Basin Ethiopia: implications for water resources and sediment transport

Moges B. Wagena [1,2] · Andrew Sommerlot [1] · Anteneh Z. Abiy [3] ·
Amy S. Collick [4] · Simon Langan [5] · Daniel R. Fuka [1] ·
Zachary M. Easton [1]

Abstract As much as 66% of the Nile River flow that reaches Egypt originates in the Highlands of the Ethiopian Blue Nile Basin (BNB). This imbalance in water availability poses a threat to water security in the region and could be impacted by climate change. This study coupled a watershed model analysis with bias corrected and downscaled Intergovernmental Panel on Climate Change (IPCC) Coupled Model Intercomparison Project 5 (CMIP5) climate data to assess the potential impact of climate change on water resources and sediment dynamics in two critical headwater basins of the BNB. Climate scenarios analyzed include RCP2.6, RCP4.5, RCP6.0, and RCP8.5 from six climate models, which were used to force watershed models calibrated against historic streamflow for six gauged sub-watersheds in the Tana basin and four gauged sub-watersheds in the Beles basin. We developed distributed watershed model parameter estimates from the gauged sub-watersheds, which were applied to un-gauged portions of the basins using topographically informed parameter transfer functions. We analyzed the impact of climate change for two future time periods (2041–2065 and 2075–2099) by running each of the six downscaled and bias corrected CMIP5 model predicted climate forcings through the watershed models to assess the impact of ensemble model mean and variance in climate change prediction on water availability and sediment transport. Results indicate that the Tana and Beles basins will experience increases both in mean annual flow (22-

---

✉ Zachary M. Easton
   zeaston@vt.edu

[1]   Department of Biological Systems Engineering, Virginia Tech, Blacksburg, VA, USA

[2]   Abay Basin Authority, Beles Subbasin Organization, Assosa, Ethiopia

[3]   Abay Basin Authority, Tana Subbasin Organization, Bahir Dar, Ethiopia

[4]   Department of Agriculture, Food and Resource Sciences, University of Maryland Eastern Shore, Princess Anne, MD, USA

[5]   International Water Management Institute, Nile Basin and East Africa, Addis Ababa, Ethiopia

27%) and sediment concentrations (16-19%). Interestingly, and of significance for water availability and hydropower development, the monsoon in the Tana and Beles basins will lengthen by approximately four (Tana) to six (Beles) weeks. These results highlight both the considerable variance in climate change impacts as well as the potential for beneficial outcomes in the region.

1 Introduction

The Ethiopian Highlands are the source of almost 90% of the flow reaching Egypt during the rainy season, and more than 66% on average (Ibrahim et al. 2009). There is a growing concern about how climate change will impact the Blue Nile Basin (BNB) water resources (Sutcliffe and Parks 1999; Arseno and Tamrat 2005). While there have been several studies of past hydroclimate variability (Conway 2000; 2005; Hulme 1994; Kebede et al. 2006; McCartney et al. 2012) and projected future changes in precipitation and temperature (Beyene et al. 2009), there are few comprehensive studies that couple climate change model output with watershed models (Adem et al. 2016) to asses water resource availability in a more mechanistic manner. These model couplings are critical to assess the impact of climate change on both regional water resources and on local impacts, such as agricultural productivity in the rain fed Ethiopian Highland system, and on landscape erosion, which could have a large impact on agricultural productivity, hydropower development and irrigation development in the basin (Hydrosult Inc et al. 2006).

Sediment is of particular concern in the BNB, where some of the highest erosion rates in the world have been documented, greater than 500 tons ha^{-1} yr^{-1} (SCRP 2000; Tebebu et al. 2010) and has the potential to impact the significant investments in hydropower and irrigation schemes. The United Nations Food and Agricultural Organization (1986) estimates annual loss of 1.9 billion tons of soil from the Ethiopian Highlands; resulting in depletion of live storage in Nile Basin reservoirs. An assessment of the impact of climate change on erosion and sediment would provide basin managers with data to incorporate into reservoir operation and irrigation planning and provide information pertinent to addressing land degradation and agricultural productivity.

The BNB already experiences significant climate variability (McCartney et al. 2012). Within the BNB, movement of air masses associated with the Inter-Tropical Convergence Zone (ICTZ) monsoon controls precipitation, resulting in pronounced wet and dry cycles. There is considerable inter-annual variability, but the BNB experiences a large range in precipitation across the basin, approximately 500 mm yr^{-1} of precipitation falls near the Sudan border to more than 2,000 mm yr^{-1} in some places in the southern basin (Awulachew et al. 2008). Potential evapotranspiration (ET) also varies considerably and is highly correlated with altitude. Near the border with Sudan, ET generally exceeds 2,200 mm y^{-1}, and during the rainy season (June to September), precipitation rarely exceeds 50% of ET. In contrast, in the highlands of Ethiopia ET ranges from approximately 1,300 to 1,700 mm y^{-1} and in many places is less than precipitation during the monsoon (McCartney et al. 2012).

As a result of the precipitation and ET cycles, stream flow in much of the BNB is characterized by extreme seasonal and inter-annual variability. At Khartoum, Sudan annual flow varies from approximately 23.0 Bm^3 to 62.6 Bm^3. Flow also varies considerably at locations along the river as measured at gauging stations maintained by the Ethiopian Ministry of Water

Resources, Irrigation, and Electricity (MoWIE). Typically, more than 80% of the flow occurs during the monsoon season (June to September) while only 4% of the flow occurs during the dry season (February to May) (Awulachew et al. 2008).

In order to better understand the implications of climate change on BNB water resources and sedimentation, we coupled outputs of six downscaled and bias corrected Coupled Model Intercomparison Project 5 (CMIP5) Global Climate Models (GCM) climate change scenarios with watershed models and assessed the response for two future time periods on the fluxes of water and sediment in the Tana and Beles basins (Fig. 1 in Online Resources). We initialized both the Tana and Beles subbasins using a modified version of the Soil and Water Assessment Tool (SWAT) model (Arnold et al. 1998) developed by Easton et al. (2008, 2010, and 2011), Fuka et al. (2016) and White et al. (2011). We analyzed individual climate model and Representative Concentration Pathways (RCP- representing four levels of total radiative forcing in Watts per square meter by 2100) scenario impacts as well as the ensemble model mean projected changes.

2 Methods and analysis

Basin descriptions The Tana basin, located in the northern headwaters of the Ethiopian BNB (Fig. 1 in Online Resources) occupies a drainage area of 14,996 km^2, and contains predominantly vertisol soils with small areas of luvisols and leptosols (Fig. 1 in Online Resources, FAO-AGL 2003). Landuse in the basin consists of pasture and crops (64%) and agro-forestry (34%) (Fig. 1 Online Resources). Elevations range from 1,781 to 4,109 m above sea level. The summer monsoon months (May to September) account for roughly 70% of the 1,345 mm in mean annual precipitation. Mean temperature is 18°C (1979–2010). The Tana basin is the source of water for the "Tana-Beles Transfer", a hydropower project that transfers stored water in Lake Tana through a tunnel system in the Beles Mountains, to take advantage of the significant pressure head difference between Lake Tana and the Beles River, generating an expected 460 MW of power.

The Beles basin abuts the Tana basin to the west-southwest and occupies a drainage area of 13,553 km^2 (Fig. 1 in Online Resources). Landuse is similar to Tana, with rain-fed agriculture in a mixed farming system, and soils are predominantly vertisols (Fig. 1 in Online Resources). Elevations range from 530 to 2450 m above sea level. The climate in the Beles basin ranges from near desert-like in the far southwest region at low elevations to tropical monsoon in the higher elevations near the Tana border. Annual average precipitation is 1,143 mm and temperature is 20°C (1979–2010).

Model description The SWAT model is a river basin model originally intended to model long-term runoff from agricultural watersheds (Arnold et al. 1998). Soils data, land use/ management information, and elevation data are required by SWAT to estimate flows and direct subbasin routing. We used a modified version of SWAT, SWAT-Variable Source Area (VSA), which has been shown to predict flow and sediment dynamics in the BNB well (Easton et al. 2008, 2010, and 2011). In SWAT-VSA each Hydrologic Response Unit (HRU) is defined by the coincidence of landuse and Topographic Index (TI) class (Easton et al. 2008), which defines areas of the landscape with respect to their hydraulic energy, and translates into runoff and erosion potential. In SWAT-VSA, the runoff for each TI class/land-use defined HRU is calculated with the re-conceptualized Curve Number method (Easton et al. 2008), and the

effective moisture storage associated with each HRU's TI class is determined by relative landscape position.

2.1 Model input data

Spatial data Tabular and spatial soil and land use information, and elevation data are required model inputs. For SWAT-VSA, we substituted an integration of the TI and soils data for the soils map to create the HRUs. SWAT requires many soil properties for both the hydrologic and sediment subroutines, thus the integration of the TI and soils involved areally weighting the FAO soils map units using the TI and extracting the associated soils properties from the FAO database. These values populated look up tables and were then linked to the map in the ArcSWAT interface (Arnold et al. 1998). We lumped the watershed's TI into 10 equal area intervals ranging from 1 to 10, with index class 1 covering the 10% of the watershed area with the lowest TI (i.e. driest or lowest probability to saturate) and index class 10 containing the 10% of the watershed with the highest TI (i.e. wettest or highest probability to saturate) (Fig. 1 in Online Resources). These TI classes were intersected with the landuse to create HRUs in each basin. Landuse layers for both models were developed by the MoWIE (Fig. 1 in Online Resources). The basin outlet for the Tana model was the Chara Chara weir in Bahir Dar, Ethiopia. For the Beles model, the basin outlet was the confluence of the Main Beles with the Blue Nile proper.

Baseline meteorological data To force the model for each of the six MoWIE flow gages the NCEP-CFSR dataset (Saha et al. 2010) was used as the meteorological forcing data set because it had a complete historical record for the time period of the MoWIE streamflow data, is of relatively high spatial resolution (38 km), and has been shown to be accurate at predicting watershed discharge in the region (Fuka et al. 2013). This dataset contains precipitation, min and max temperatures, humidity, wind speed and solar radiation for each hour for any land location in the world. For each basin we interpolated the CFSR data to the center of the basin.

Estimation of model parameters and calibration We initialized and calibrated SWAT-VSA for each of the MoWIE stream gages located in the Tana and Beles basins. We utilized only those gages with reliable flow and sediment data between 1998 and 2010. The SWAT-CUP (SWAT Calibration and Uncertainty Procedure) model was used for model parameter estimation, verification, sensitivity, and uncertainty analysis. Model parameters were calibrated using the SUFI2 (Sequential Uncertainty Fitting) model. The objective function used for calibration was the Nash-Sutcliffe (Nash and Sutcliffe 1970) coefficient (NS). Tables 1-2 in Online Resources give fitted model parameters and model calibration/verification results.

To better capture the landscape and climate variability across the two basins, we calibrated the models at six internal sub-watershed locations with flow and sediment data (Fig 1 In Online Resources). These calibrated sub-watersheds were then used to develop distributed watershed model parameter estimates from the gauged sub-watersheds, which were applied to un-gauged portions of the basins using topographically informed parameter transfer functions. This approach allowed variation in input data between basins, as opposed to a global calibration performed at the basin outlet. CMIP5 data are then applied to each sub-watershed in the model via an inverse distance squared procedure from the CMIP5 model

grid, interpolated to the centroid of each basin. Thus, the results in Tables 1 and 2 and Figs. 1, 2, 3 and 4 represent the integrated basin response that takes into account the distribution of calibrated model parameters and CMIP5 predictions.

We calibrated all models first for daily flow followed by a monthly flow and sediment calibration from 1998 to 2001 and corroborated all models from 2002 to 2005. The daily flow calibration followed by the monthly calibration was necessary because some of the sediment data was only available at the monthly time step and there are model parameters that influence both flow and sediment simultaneously.

Incorporating climate change scenarios The CMIP5 dataset, obtained from the Earth System Grid Federation (https://esgf-data.dkrz.de/projects/esgf-dkrz/), includes four RCP

Table 1 Base case, ensemble minimum, mean, maximum and percentage change (from the base case) in discharge and sediment concentration for the climate change scenarios for the Tana subbasin by month for the two future time frames

Month	Base	2041-2065			2075-2099		
	1979-2010	Min	Mean	Max	Min	Mean	Max
Discharge (m3/s)							
January	39	50	57	67	49	57	67
February	29	41	45	49	41	44	49
March	29	41	44	52	40	43	49
April	35	52	57	64	49	56	65
May	46	65	80	98	66	79	97
June	96	99	153	213	99	153	214
July	278	218	315	419	218	310	410
August	415	425	456	465	416	448	460
September	332	301	388	462	303	389	459
October	176	190	241	296	196	245	298
November	93	111	145	186	114	150	192
December	57	70	87	109	67	88	112
% Change		2	27	53	2	27	57
Sediment Concentration (mg/kg)							
January	15	17	18	19	17	17	18
February	13	16	16	17	16	16	17
March	14	16	18	21	16	17	19
April	15	20	21	22	19	21	23
May	18	22	24	26	23	24	26
June	24	26	30	33	27	30	33
July	34	33	37	40	33	37	40
August	38	40	40	40	40	40	40
September	32	32	36	40	32	36	40
October	25	28	30	32	28	30	32
November	20	22	25	28	22	25	28
December	16	19	20	22	18	20	22
% Change		11	19	28	10	18	28

Table 2 Base case, ensemble minimum, mean, maximum and percentage change (from the base case) discharge and sediment concentration for the climate change scenarios for the Beles subbasin by month for the two future time frames

Month	Base 1979-2010	2041-2065			2075-2099		
		Min	Mean	Max	Min	Mean	Max
Discharge (m3/s)							
January	3	3	8	17	3	8	19
February	0	1	1	2	1	2	3
March	2	1	4	10	1	4	9
April	5	9	12	22	9	14	23
May	44	31	84	139	25	91	139
June	153	135	228	332	142	231	326
July	409	339	499	709	332	488	686
August	802	723	894	1041	700	863	1017
September	852	763	903	1037	755	895	1016
October	447	398	591	757	420	603	749
November	137	108	222	383	120	238	405
December	21	14	49	102	16	55	114
% Change		−12	22	58	−12	21	57
Sediment Concentration (mg/kg)							
January	6	7	10	14	7	10	15
February	4	5	5	6	5	6	7
March	9	6	13	20	6	12	18
April	11	16	18	22	17	20	24
May	22	27	32	36	25	32	36
June	30	34	37	41	35	38	40
July	41	41	44	47	40	43	46
August	50	46	47	47	45	46	47
September	52	46	47	48	47	48	49
October	41	41	45	47	41	45	48
November	26	28	34	40	28	35	40
December	12	12	20	27	12	21	28
% Change		1	16	31	1	17	31

scenarios: RCP2.6 (peak in radiative forcing at 2.6 W/m^2 before 2100 and decline thereafter); RCP4.5 (stabilization without overshoot to 4.5 W/m^2 at 2100); RCP6 (stabilization without overshoot to 6 W/m^2 after 2100); RCP8.5 (increasing radiative forcing to 8.5 W/m^2 by 2100). We selected and evaluated six GCMs based on the work of Bhattacharjee and Zaitchik (2015) [CCSM4, CSIRO-Mk3.6.0, GFDL-ESM2M, MEROC5, HadGEM2-ES, and IPSL-CM5A-LR models (Online Resources Table 3)], who verified that these GCM's adequately capture the mean, variability and the seasonality of precipitation in BNB. The GCM's were downscaled to a 0.5-degree resolution (~50 km) to the centroid of each sub-watershed for the time periods of 1979–2005 (historical period) and 2041–2065 and 2075–2099 for future projections. These data were downscaled using bias correction-spatial disaggregation methods adapted to a daily time series in R following Girvetz et al. (2013) using functions from the
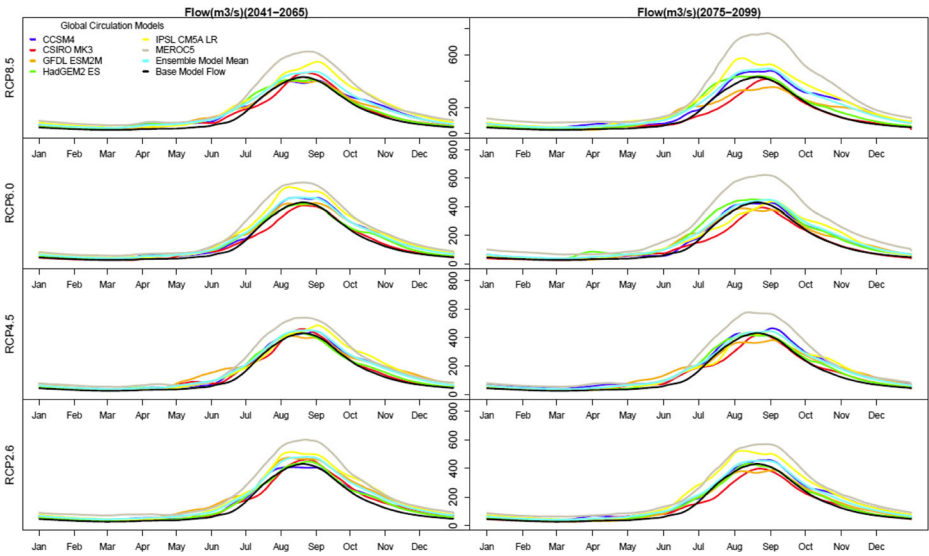
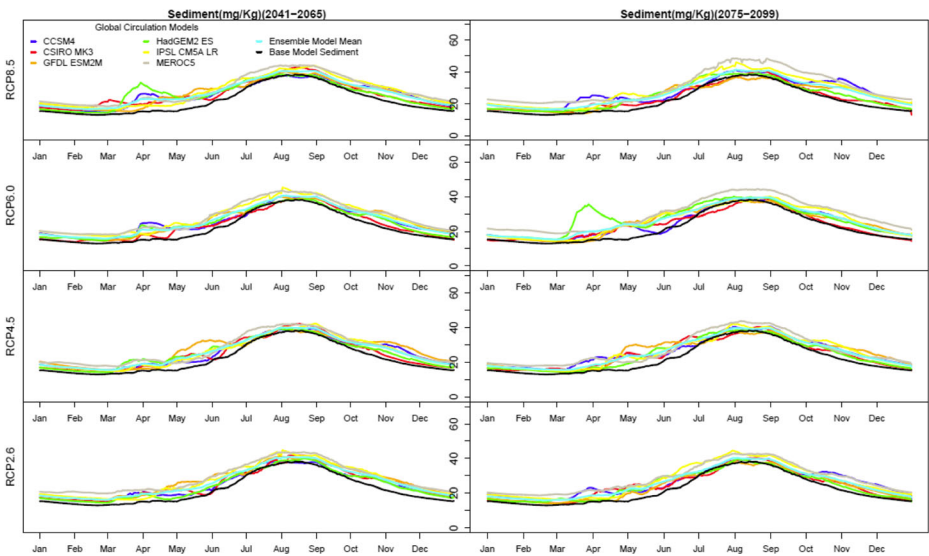**Fig. 1** Observed historical and predicted average-by-day discharge for the Tana subbasin at the Chara Chara weir in Bahidar Ethiopia for the four emissions scenarios and two future 25 yr time periods for each climate model

QMAP R package (Gudmundsson et al. 2012). The downscaling method assumes no parametrically defined distribution shape, but rather defines separate linear interpolation mapping functions for each empirical quantile of the cumulative distribution function of the historical data (Boé et al. 2007). The goal of the method is to make the modeled data statistically similar to the historical reference data while preserving the characteristics of the model data. In total, three

Fig. 2 Observed historical and predicted average-by-day sediment concentrations for the Tana subbasin Chara Chara weir in Bahidar Ethiopia for the four emissions scenarios and two future 25 yr time periods for each climate model
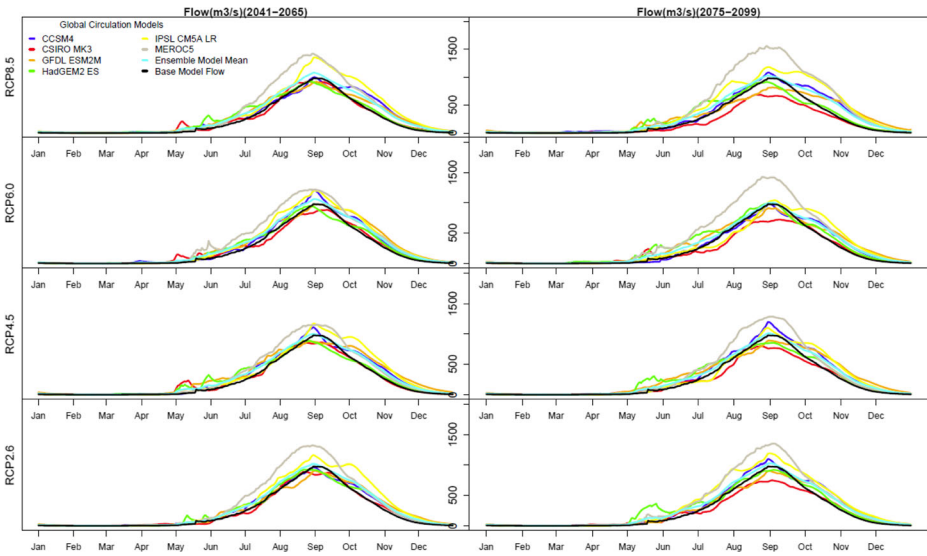
Fig. 3 Observed historical and predicted average-by-day discharge for the Beles subbasin at the confluence with the Blue Nile for the four emissions scenarios and two future 25 yr time periods for each climate model

separate data sets are needed to complete the procedure: historical data as a downscaling reference, historical data from the climate model source, and future, or predicted data from the climate model source. The mapping functions defined by each quantile of historical reference and historical modeled data are applied to the future modeled data. The accuracy of the historical, bias corrected CMIP5 data from each of the models was verified by employing the Equiratio Cumulative Distribution Function (ECDF) matching method (Li et al. 2010; Wang and Chen 2014) against
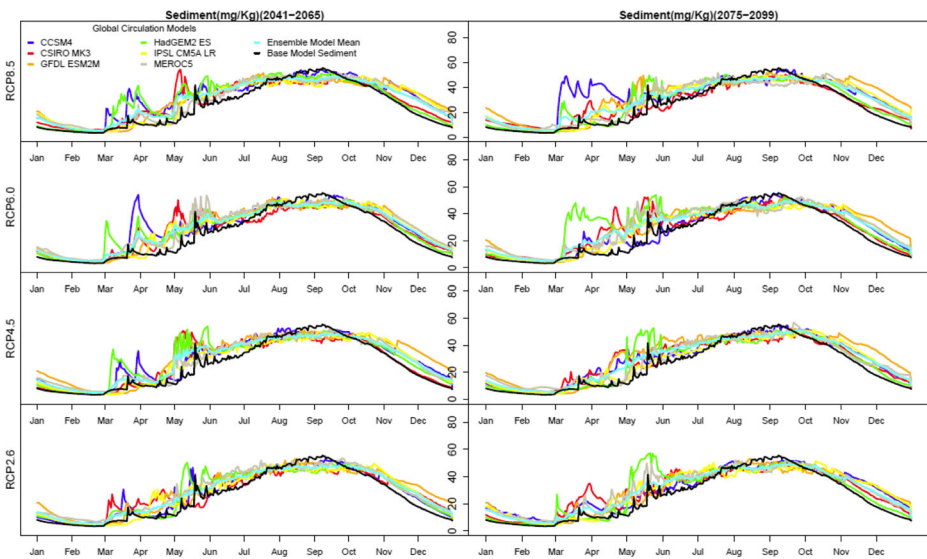

Fig. 4 Observed historical and predicted average-by-day sediment concentrations for the Beles subbasin at the confluence with the Blue Nile for the four emissions scenarios and two future 25 yr time periods for each climate model

the historical CFSR dataset. (ECDF plots are shown in Online Resources Figs. 2-13). More information on the downscaling can be found in Online Resources

3 Results

The results of model calibration and verification are shown in Table 2 (Online Resources) and indicate that for almost all sub-watersheds the models predicted discharge adequately. The one exception is for the Ribb sub-watershed during the verification period, which is poor for daily but acceptable for monthly verification (Table 2 Online Resources). This is likely due to an error in measured flow as measured discharge was greater than precipitation during that period. Removing this period from the verification data set results in a daily NS of 0.36. Sediment data was available for the Beles at a daily time step for both the calibration (1998–2001) and verification (2002–2005) periods, while Tana only had monthly sediment concentration measurements for the calibration and verification periods. Both the Tana and Beles models predicted sediment concentrations suitably well (Table 2 Online Resources).

Using these models we incorporated the climate change scenarios for each of the two future time periods. Results of the individual climate models for each RCP scenario are presented on an average by day basis in Figs. 1 and 2 for Tana and Figs. 3 and 4 for Beles. Tables 1 and 2 present the mean, minimum, maximum and percentage change from the base case for monthly flow and sediment concentrations for each basin and future time period as predicted by the SWAT-VSA model for the ensemble climate model mean. Online Resources Tables 3-7 present the climate change scenario results for each individual IPCC Fifth Assessment Report (AR5) scenario and future time period (average of the six GCMs for each AR5 scenario). Together these results provide insight into how the variation in climate model predictions propagate through the watershed models to influence water resources and sediment dynamics in the two basins as well as how the model ensemble performs.

Changes in precipitation and temperature An analysis of future changes in precipitation and temperature in the Beles basin showed that the mean annual precipitation increases by 11.0% with a standard deviation of 33.4% across all climate models in the 2041–2065 period, and 11.7% with a standard deviation of 29.4% across all climate models in the 2075–2099 period. Maximum and minimum temperature increases by a mean of 8.6% and 18.0%, respectively with standard deviations of 0.2% and 9.5%, respectively across all models during the 2041–2065 period and during the 2075–2099 period maximum and minimum temperatures increases by 2.4% and 24.5%, respectively with standard deviations of −4.5% and 20.1%, respectively across all models. In Tana precipitation increases by a mean of 17.6% with standard deviation of 35.0% across all climate models in the 2041–2065 period and 18.4% with a standard deviation of 25.3% across all climate models in the 2075–2099 period. Maximum and minimum temperature increases by a mean of 15.7% and 25.5% with standard deviation of −16% and 20.1%, respectively across all models during the 2041–2065 period, and during the 2075–2099 period maximum and minimum temperatures increases by 21.2% and 34.7%, respectively with standard deviations of −20.2% and 20.1%, respectively across all models.

Tana flow Figure 1 presents the result of the climate change scenario analysis for flow in the Tana basin. Almost all models predict increases in mean annual flow for both future time periods. The exception to this is a slight predicted decrease from the CSIRO-MK3 model under all scenarios for the 2075–2099 time period and the GFDL-ESM2M model under the RCP4.5, RCP6.0, and RCP8.5 scenarios for the 2075–2099 time period. The ensemble model projections (Fig. 1) predict either an increase in flow or no change from the base period across all time periods and RCP scenarios. The MEROC5 model predicted the largest flow increases; nearly 100% more flow during the monsoon peak in July-September, for the 2075–2099 time period and the RCP6.0 and RCP8.5 scenarios (Fig. 1). The other climate models predicted both peak and baseflow to increase under all scenarios for both time periods, although substantially less than the MEROC5 model (Fig. 1).

Table 1 presents the mean, min and max change in flow by month of the aggregate AR5 scenarios (e.g., each climate model and RCP scenario averaged together after it has been run through the model) as well as the percent change from the base period. The ensemble model mean predicts 27% more flow during both time periods, the range in projected change is +2% to +57%. The climate models generally predicted an increase in the peak discharge in July-September, across all RCP scenarios and time periods except for CSIRO-MK3 and GFDL-ESM2M models, which predicted decreases during the July-September peak (Fig. 1).

Across time periods, both the RCP2.6 and RCP6.0 scenarios have greater increases in flow during 2041–2065 (29% and 27%) than 2075–2099 (23% and 25%), while the RCP8.5 scenario predicted the largest increase in flows (+38%) to occur during the 2075–2099 time period. The RCP4.5 scenario predicted a 22% increase in flow in both the 2041–2065 and 2075–2099 time periods (Online Resources Table 4).

Table 1 shows an increase in the discharge for all months during both periods and the largest proportional increases occur from June to November. The results indicate a significant increase in the length of the monsoon, (generally occurring from May to late September, lengthening to April to November) and in the total flow.

Tana sediment Figure 2 presents the predicted sediment concentrations for individual climate models and RCP scenarios in the Tana basin. Similar to the projected increase in flow, sediment concentrations increase on an annual average basis (+19% 2041–2065 and +18% 2075–2099, Table 1). There are early (April) and late (November) season increases in concentrations predicted by the HadGEM2ES, CCSM4, GFDL-ESM2M, and CSIRO-MK3 models that coincide with increases in flow predicted by those models. This is primarily due to a shift in precipitation and precipitation intensity to earlier in the year. The model mean projections (Table 1, Fig. 2) indicate that on average sediment concentrations will increase during all times of the year, but particularly during the early and late monsoon. Mean annual sediment concentration increases range from 17 to 22% (Table 1).

Across time periods, both the RCP2.6 and RCP8.5 scenarios have greater increases in sediment concentrations during 2041–2065 (19% and 22%) than 2075–2099 (17% and 21%). Both the RCP4.5 and RCP6.5 scenarios predicted no difference between the concentrations in the 2041–2065 and 2075–2099 time periods, 17% and 18%, respectively (Online Resources Table 5).

Beles flow Figure 3 shows the results for flow for the Beles basin. While average annual flows are projected to increase for all models and RCP scenarios during the 2041–2065 period (Table 2), there is considerable variation in the seasonal dynamics of that increase. For

instance, the CISRO-MK3, GFDL-ESM2M, and HadGEM2-ES models show a decrease in flow during the peak, and a shift to greater early and late season flows (Fig. 3), while the MEROC5, IPSL-CM5A-LR, and CCSM4 models predict substantial peak flow increases across all RCP scenarios (Fig. 3). During the 2075–2099 time period the trend is similar, decreases in peak flows for the HadGEM2ES, CSIRO-MK3, and GFDL-ESM2M models, and greater early and late season flow (Fig. 3). Here however, the magnitude of those changes is amplified relative to the 2041–2065 period, particularly for the RCP6.0, and RCP8.5 scenarios. The MEROC5 and IPSL-CM5A-LR models predict peak flow increases across all RCP scenarios, while the CCSM4 model predicts peak flow increases for the RCP2.6 and 4.5 scenarios (Fig. 3). Discharge increases are greatest for RCP8.5 during both scenario periods (+26% and +27%, respectively), while discharge increases are lowest during 2041–2065 and 2075–2099 for the RCP2.6 and RCP4.5, +18% for both (Online Resources Table 6). Table 2 shows a large range in predicted discharge (−12 to +58%, mean +22% for 2041–2065 and −12% to +57 %, mean +27% for 2075–2099) and a moderate lengthening of the monsoon.

Beles sediment Figure 4 presents the model results for sediment concentrations for all climate models and RCP scenarios. Sediment concentrations increase in both time periods, and there is a significant increase in early and late season concentrations while decreases occur during the monsoon peak (June to August) (Fig. 4). The increase is particularly variable during the early season where increases range from 15 to 300% during April-June. This early season sediment increase is due to increased precipitation intensity (increases of 5.7-45.7% from April to June) predicted by the models coinciding with tillage of the highly erodible soils in the region.

Increases in sediment concentrations are greatest for RCP8.5 during both time periods (+18%, Table 2). The RCP2.6 scenario predicts the lowest sediment concentrations during the 2041–2065 period (+14%) (Online Resources Table 7). On a mean annual basis, sediment concentrations are predicted to increase 16% for the 2041–2065 periods and 17% for the 2075–2099 period although there is a considerable range between the different scenarios (+1% to +31% for both 2041–2065 and 2075–2099, Table 2).

4 Discussion

Climate change in portions of the BNB of Ethiopia has the potential to significantly alter flow and sediment regimes. Our results suggest that both the Tana and Beles basins have the potential for significantly increased flow. While there is a tendency for increased precipitation intensity, particularly early in the monsoon (which is primarily responsible for the proportionally greater sediment loss during that period), the majority of the increase in flow is due to frontal type orographic storms. These results differ to some extent from Taye et al. (2015) who found significantly higher precipitation intensities using the IPCC Fourth Assessment Report (AR4) climate data. Dile et al. (2013), using SWAT and AR4 climate data, predicted similar annual increases in flow as our analysis revealed in the Gilgel Abay basin (a sub-watershed in Tana), but increases during the peak were much greater (+50%) than our results suggest. There were subsequent decreases in flow during the later period of the monsoon (Dile et al. 2013), which the AR5 data used in this analysis did not show.

Tana can expect to experience an increase in total discharge and in the length of high flow period. The Beles basin is predicted to likewise experience an increase in discharge although

there is more variability in the timing of these changes. For instance, the higher emissions scenarios RCP6.0 and RCP8.5 offer perhaps the best-case results for Tana discharge (+25% to +38%, Table 4 in Online Resources). This increase has several beneficial outcomes for the region: 1) increased development potential of irrigation projects in the basin; 2) increased hydroelectric energy generation potential in the Tana-Beles transfer, currently 2,420 Mm^3 yr^{-1} (McCartney et al. 2012); 3) increased environmental flows from Tana could ensure downstream ecosystem productivity; and 4) increased inflow to the Grand Ethiopian Renaissance Dam currently under construction on the main stem of the Blue Nile River in Ethiopia (King and Block 2014). Indeed, discharge from the Tana basin over the Chara Chara weir via the main stem of the Blue Nile is predicted to increase from 136 m^3/s currently to 172 m^3/s during both future time periods.

The lengthening of the monsoon period in both basins could also result in increased water availability for rain-fed agricultural, domestic consumption and habitat. Sudan and Egypt would benefit from the increased flow but would have to deal with increased sediment loads in their reservoir operations (note that both Sudan and Egypt depend on upstream sediment to replenish field soils, so not all of the predicted increase in sediment is negative). The increase in peak flow during July-September in the Tana basin could increase the water level of lake and potentially inundate flood plains causing severe damage to crops that would be nearing maturity (Woubet 2007). However, this flooding (particularly in Fogera plain where the Ribb and Gumera rivers drain into Lake Tana and in the Dembiya plain where Dirma and Megech rivers enter the lake) may increase rice farming and productivity, an important source of income for farmers in the region (Haileslassie et al. 2009). Wetlands on the eastern side of Lake Tana, which provide habitat for several unique and threatened species, could also be regenerated; they are currently shrinking due to over pumping of water for irrigation (Dejen et al. 2011).

The increases in sediment pose a larger problem, as sediment is particularly deleterious for reservoir operations due to reduced live storage and for hydropower generation and irrigation. This is of a particular concern for the Grand Renaissance Dam under construction in Ethiopia. However, reservoir operations could be modified to avoid the highest concentration flows while still retaining adequate flows to fill the reservoirs. For instance, avoiding the early season flows that have higher sediment concentrations. To reduce sediment delivery, soil conservation practices at erosion prone areas of the basin could reduce the rate, amount, and subsequent delivery of eroded material to the reservoirs (Tebebu et al. 2010).

The results for the Beles basin indicate a relatively large change in average annual flow and substantial increases in sediment concentrations during early and late season. However, most models suggest a decrease in sediment concentration during peak monsoon (June to September). There is only one planned large-scale hydropower reservoir (Danguar Dam, McCartney et al. 2012) in the Beles that would suffer from the increase in sediment, and operations may be able to avoid retaining the early and late flows with high sediment concentrations and instead retain the peak flows, which are lower in sediment (Fig. 4).

Planned irrigation schemes in Beles to irrigate a command area of more than 135,000 ha (the largest irrigation development proposed in the upper Blue Nile- McCartney et al. 2012) may suffer from this increase in sediment, which can damage pumps and clog irrigation pipe and canals. Again timing of activities will be critical. For instance, diversions will not likely occur during the monsoon as ample precipitation falls in the region, but rather will be developed to extend the growing season at either end of the monsoon. Unfortunately, sediment concentrations are substantially higher during the early and late season. However, the

predicted increase in discharge in Beles is primarily a result of increased early and late season precipitation, making irrigation less critical.

For agricultural productivity, the results are quite promising. The longer monsoon (Figs. 1 and 3) will afford the possibility of double cropping in much of the region, and increased soil moisture will reduce crop drought stress. However, increased erosion rates could eventually threaten the possibility of increased crop productivity by removing valuable topsoil and nutrients from fields, and reducing the water holding capacity of the soil. Some of this increase in erosion could be avoided by adjusting the timing of the major field tillage operations to coincide with less intense precipitation. Measures to maintain soil cover (e.g., cover crops, conservation tillage) could help to reduce erosion and even conserve soil moisture (Ogle et al. 2005), ultimately increasing system productivity.

5 Conclusions

Climate change in the BNB of Ethiopia is predicted to significantly alter basin level discharge, under all RCP scenarios. Discharge in both basins is projected to increase, in some cases substantially, depending on the RCP scenario, model, and time frame. The ensemble model mean results suggest increases of 27% in Tana and 21-22% in Beles are likely. Consequently, sediment concentrations are predicted to increase, particularly during the early and late portion of the monsoon, and in some cases to decrease during the peak monsoon. These results suggest that reservoir operation, flood management, and irrigation scheme development should consider the impacts of climate change to mitigate negative consequences of changes in discharge and sediment in both basins. Agricultural producers although possibly benefiting from increased precipitation will be challenged with increased landscape erosion and should consider practices to control erosion.

References

Adem AA, Tilahun SA, Ayana EK, Worqlul AW, Assefa TT, Dessu SB and Melesse AM (2016) Climate Change Impact on Sediment Yield in the Upper Gilgel Abay Catchment, Blue Nile Basin, Ethiopia Landscape Dynamics, Soils and Hydrological Processes in Varied Climates (pp. 615–644): Springer

Arnold JG, Srinivasan R, Muttiah RR, Williams JR (1998) Large area hydrologic modeling and assessment part I: model development. J Am Water Resour Assoc 34(1):73–89

Arseno Y, Tamrat I (2005) Ethiopia and the eastern Nile Basin 16:15–27

Awulachew SB, MP McCartney TS. Steenhuis AA. Ahmed. (2008) A review of hydrology, sediment and water resource use in the Blue Nile Basin. International Water Management Institute Report

Bhattacharjee P, Zaitchik B (2015) Perspectives on CMIP5 model performance in the Nile river headwaters regions. Int J Climatol. doi:10.1002/joc.4284

Beyene T, Lettenmaier D, Kabat P (2009) Hydrologic impacts of climate change on the Nile river basin: implications of the 2007 IPCC scenarios. Climate Change 100(3–4):433–462

Boé J, Terray L, Habets F, Martin E (2007) Statistical and dynamical downscaling of the seine basin climate for hydro-meteorological studies. Int J Climatol 27(12):1643–1655

Conway D (2000) The climate and hydrology of the upper blue Nile river. Geogr J 166:49–62

Conway D (2005) From headwater tributaries to international river: observing and adapting to climate variability and change in the Nile basin. Glob Environ Chang 15:99–114

Dejen E, Vijverberg J, Atnafu N (2011) Assessment of the ecological status and threats of welala and shesher wetlands lake tana Sub-basin (Ethiopia). J Water Resour Prot 3:540–547

Dile Y, Berndtsson R, Setgen S (2013) Hydrological response to climate change for gilgel abay river, in the lake tana basin - upper blue Nile basin of Ethiopia. PLoS One 8(10):e79296. doi:10.1371/journal.pone.0079296

Easton ZM, Fuka DR, Walter MT, Cowan DM, Schneiderman EM, Steenhuis TS (2008) Re-conceptualizing the soil and water assessment tool (SWAT) model to predict runoff from variable source areas. J Hydrol 348: 279–291

Easton ZM, Fuka DR, White ED, Collick AS, Ashagre BB, McCartney M, Awulachew SB, Ahmed AA, Steenhuis TS (2010) A multi basin SWAT model analysis of runoff and sedimentation in the blue Nile. Ethiopia Hydrol Earth Syst Sci 14(1827–1841):2010. doi:10.5194/hess-14-1827-2010

Easton ZM, Walter MT, Fuka DR, White ED, Steenhuis TS (2011) A simple concept for calibrating runoff thresholds in quasi-distributed variable source area watershed models. Hydrol Proc. doi:10.1002/hyp.8032

FAO-AGL: WRB Map of World Soil Resources (2003) Land and Water Development Division, Food and Agriculture Organization of the United Nations. Available at: http://www.fao.org/ag/agl/agll/wrb/soilres.stm, last access: June 2010

Fuka DR, MacAllister CA, Degaetano AT, Easton ZM (2013) Using the climate forecast system reanalysis dataset to improve weather input data for watershed models. Hydrol Proc. doi:10.1002/hyp.10073

Fuka D.R., A.S. Collick, P. Kleinman, D. Auerbach, D, Harmel, Z.M. Easton. 2016. Improving the spatial representation of soil properties and hydrology using topographically derived initialization processes in the SWAT model. Hydrol Proc. doi:10.1002/hyp.10899

Girvetz EH, Duffy P, Ruesch A, Thrasher B, Zganjar C (2013) Making climate data relevant to decision making: the important details of spatial and temporal downscaling 1–43. World Bank 27:43

Gudmundsson L, Bremnes JB, Haugen JE, Engen-Skaugen T (2012) Technical note: downscaling RCM precipitation to the station scale using statistical transformations - a comparison of methods. Hydrol and Earth Sys Sci 16:3383–3390. doi:10.5194/hess-16-3383-2012

Haileslassie A, Peden D, Gebreselassie S, Amede T, Descheemaeker K (2009) Livestock water productivity in mixed crop–livestock farming systems of the blue Nile basin: assessing variability and prospects for improvement. Agric Syst 102:33–40

Hulme M (1994) Global climate change in the Nile basin. In Eds. Howell, P.P. and Allan, J.A. The Nile: Sharing a scarce resource. Cambridge Univ Press. ISBN 0 521 45040 3

Hydrosult Inc, Tecsult, DHV and their Associates Nile Consult, Comatex Nilotica and T and A Consulting (2006) Trans-boundary analysis: Abay – Blue Nile Sub-basin. NBI-ENTRO (Nile Basin Initiative-Eastern Nile Technical Regional Organization)

Ibrahim YA, Ahmed AA, Ramdan MS (2009) Improving Water Management Practices in the Rahad Scheme (Sudan). In: Awulachew, S.B. T. Erkossa, V. Smakhtin, F. Ashra. Improved water and land management in the Ethiopian highlands: its impact on downstream stakeholders dependent on the Blue Nile. Addis Ababa, Ethiopia. 5–6 February 2009

Kebede S, Travi Y, Alemayehu T, Marc V (2006) Water balance of Lake Tana and its sensitivity to fluctuations in rainfall, Blue Nile basin, Ethiopia. J Hydrol 316:233–247. doi:10.1016/j.jhydrol.2005.05.011

King A, Block P (2014) An assessment of reservoir filling policies for the grand Ethiopian renaissance Dam. J Water Climate Change 5:233–243

Li H, Sheffield J, Wood EF (2010) Bias correction of monthly precipitation and temperature fields from intergovernmental panel on climate change AR4 models using equidistant quantile matching. J Geophys Res. doi:10.1029/2009JD012882

McCartney MT, Alemayehu Y, Seleshi, Shiferaw YA, Ibrahim ZM, Easton, and Awulachew SB (2012) Simulating current and future water resource development in the Blue Nile River Basin. In S.B. Awulachew, V. Smakhtin, D. Molden and D. Peden, eds. The Nile River Basin: Water, Agriculture, Governance and Livelihoods. Earthscan Publishing. Nov 5. 344 pgs.

Nash JE, Sutcliffe JV (1970) River flow forecasting through conceptual models part I a discussion of principles. J Hydrol 10:282–290

Ogle SM, Brandt FJ, Paustain K (2005) Agricultural management impacts on soil organic carbon storage under moist and dry climatic conditions of temperate and tropical regions. Biogeochemistry 2(1):87–121

Saha S, Moorthi S, Pan H-L, Wu X, Wang J, Nadiga S, Tripp P, Kistler R, Woollen J, Behringer D, Liu H, Stokes D, Grumbine R, Gayno G, Wang J, Hou Y-T, Chuang H-Y, Juang H-MH, Sela J, Iredell M, Treadon R, Kleist D, Van Delst P, Keyser D, Derber J, Ek M, Meng J, Wei H, Yang R, Lord S, Van den Dool H, Kumar A, Wang W, Long C, Chelliah M, Xue Y, Huang B, Schemm J-K, Ebisuzaki W, Lin R, Xie P, Chen M, Zhou S, Higgins W, Zou C-Z, Liu Q, Chen Y, Han Y, Cucurull L, Reynolds RW, Rutledge G, Goldberg M (2010)

The NCEP climate forecast system reanalysis. Bull Am Meteorol Soc 91:1015–1057. doi:10.1175/2010 bams3001.1

SCRP (Soil Conservation Reserve Program) (2000) Area of Anjeni, Gojam, Ethiopia: Long-term monitoring of the agricultural environment 1984–1994, 2000 Soil Erosion and Conservation Database, Soil Conservation Research Programme. Centre for Development and Environment in association with the Ministry of Agriculture, Ethiopia, Berne, Switzerland

Taye MT, Willems P, Block P (2015) Implications of climate change on hydrological extremes in the blue Nile basin: a review. J Hydrol Reg Stud 4:280–293

Tebebu TY, Abiy AZ, Zegeye AD, Dahlke HE, Easton ZM, Tilahun SA, Collick AS, Kidnau S, Moges S, Dadgari F, Steenhuis TS (2010) Surface and subsurface flow effects on permanent gully formation and upland erosion near lake tana in the northern highlands of Ethiopia. Hydrol Earth Syst Sci 14:2207–2217. doi:10.5194/hess-14-2207-2010

Wang L, Chen W (2014) Equiratio cumulative distribution function matching as an improvement to the equidistant approach in bias correction of precipitation. Atmos Sci Lett 15:1–6

White ED, Easton ZM, Fuka DR, Collick AS, Adgo E, McCartney M, Awulachew SB, Selassie YG, Steenhuis TS (2011) Development and application of a physically based landscape water balance in the SWAT model. Hydrol Proc 25(915–925):2011. doi:10.1002/hyp.7876

Woubet G (2007) Flood Hazard and Risk Assessment in Fogera Woreda using GIS & Remote Sensing. Proceedings of the Workshop on Hydrology and Ecology of the Nile River Basin under Extreme Conditions, Addis Ababa, Ethiopia (2008), pp. 331–361